Advanced Diagnosis of Bearing Defects: A Multi-Domain Approach

Vinayak V. Kulkarni [1,*] and Shylesha Channapattana [2]

[1] Department of Mechanical Engineering, Karnatak Law Society's Gogte Institute of Technology, Belagavi, Visvesvaraya Technological University, Karnataka, India
[2] Department of Mechanical Engineering, Karnatak Law Society's Vishwanathrao Deshpande Institute of Technology, Haliyal, Visvesvaraya Technological University, Karnataka, India
Email: vk@git.edu (V.V.K.); shylesha@gmail.com (S.C)
*Corresponding author

***Abstract*—Early fault identification in rolling-element bearings is critical for averting failures. While measuring overall vibration levels at the bearing housing offers a simple diagnostic method, spectrum analysis provides a more advanced and precise early warning. This study introduces an innovative approach to detecting, analyzing, and diagnosing bearing defects by comparing time-domain, frequency-domain, and spectrum plot analyses. By examining spectral variations under normal conditions and in the presence of outer and inner race faults, this research enhances the accuracy and reliability of fault diagnosis.**

***Keywords*—detection of rolling element bearing flaws, time domain, frequency domain, spectrum plot approaches**

I. Introduction

Early diagnosis of faults in rolling element bearings is crucial to prevent catastrophic failures in rotating machinery. Various vibration analysis techniques have been employed to diagnose bearing defects, with methods primarily categorized into three techniques that are: time-domain form, frequency-domain form, and time-frequency form. The vibration spectrum obtained for different rotating machinery problems is analyzed using techniques such as Fast Fourier Transform (FFT) [1–6], Short-Time Fourier Transform (STFT) [5–8], and Wavelet Transform [8, 9]. These methods facilitate the identification of frequency components and their variations with amplitude in terms of acceleration, velocity, and displacement.[10] Additionally, advanced techniques like Kurtogram analysis and Artificial Neural Networks (ANNs) are being increasingly utilized for condition monitoring [11]

A. Research Gap

Despite the widespread use of vibration analysis techniques, existing studies primarily focus on either time-domain or frequency-domain methods in isolation. Limited research has provided a comprehensive comparison of these approaches alongside spectrum plot analysis for rolling element bearing fault detection. Moreover, recent advancements in signal processing and machine learning-based diagnostics have not been fully integrated into traditional vibration analysis frameworks, leaving gaps in early and accurate fault detection [9, 12]. The lack of a unified approach limits the effectiveness of condition monitoring systems, particularly under varying load and speed conditions.

B. Problem Statement

Rolling element bearings are subject to wear and failure due to continuous operational stresses, leading to unexpected breakdowns and costly maintenance. Traditional vibration analysis techniques, which rely on either time-domain or frequency-domain methods alone, may not offer a holistic diagnostic framework. This study aims to bridge this gap by systematically comparing time-domain, frequency-domain, and spectrum plot-based analyses to enhance fault detection accuracy. By incorporating recent advancements in vibration analysis, including enhanced spectral analysis techniques and intelligent diagnostic models, this research provides a more comprehensive and reliable approach for diagnosing rolling element bearing defects [10–12].

Numerous vibration analysis techniques are applied to examine rolling element faults and rotating machinery vibrations, and these methods are categorized into three primary domains: time, frequency, and time-frequency. Theoretical Basis for Time-Frequency Analysis:

- The Short-Time Fourier Transform (STFT) was applied to analyze transient fault signals [5].
- Wavelet Transform (WT) provided improved frequency resolution, especially for non-stationary signals [6].
- Envelope Analysis helped extract defect-related amplitude modulations, isolating bearing faults efficiently [8].

The time-domain method remains the simplest approach for vibration-based analysis, Including peak-to-peak amplitude values for both positive and negative cycles [13].

Manuscript received January 23, 2025; revised February 21, 2025; accepted April 10, 2025; published August 6, 2025.

The Short-Time Fourier Transform separates the vibration spectrum into short windows, whereas the Fast Fourier Transform extracts frequencies depending on their exact ranges. [14]. Additionally, the Wavelet Transform technique provides more accurate temporal resolution for high-frequency components compared to STFT [8, 9].

For rolling element bearing defects, improved methods such as the Kurtogram are also utilized [14, 15]. The Kurtogram technique aids in analyzing mixed vibration signals with frequency components using fuzzy logic systems, artificial neural networks (ANNs), and other neural network applications. These approaches are increasingly being implemented for diagnosing rotating equipment and rolling element bearing issues [11, 16]. Furthermore, neural networks play a crucial role in detecting and diagnosing defects in rotating equipment using various methodologies, with feed-forward networks being the most applied approach [17].

This study contributes to the field by systematically comparing different vibration analysis techniques and integrating contemporary advancements, ultimately enhancing the accuracy and reliability of rolling element bearing fault diagnosis.

II. Literature Review

Rolling element bearings are crucial parts in rotating machinery, and early identification of their shortcomings is crucial for preventing system failures.

Vibration analysis is one of the most widely used techniques for fault detection, with various methods focusing on both time and frequency domains. studies have shown that regularly measuring vibration levels at the bearing housing can provide early signs of faults, while more detailed spectrum analysis is often required for earlier detection [1, 2]. The use of advanced techniques such as enhanced Kurtogram method [14] and wavelet cross-spectrum analysis [10] has further improved the accuracy of fault diagnosis.

Additionally, researchers have explained the machine learning methodologies, such as support vector machines and convolutional neural networks, to enhance diagnostic abilities under varied load and speed conditions [9, 12]. Practical applications, like the MAXBE project [4], have provided insights into the real-world implementation of these methods, highlighting their effectiveness in condition monitoring systems. These studies collectively demonstrate the growing potential of combining traditional vibration analysis with advanced computational techniques for more accurate and reliable bearing fault detection.

Theoretical Basis: Time-Frequency Analysis and Non-Stationary Signal Processing

Vibration signals from rotating machinery, such as rolling element bearings, are often non-stationary, i.e., their statistical properties change over time. To analyze such signals, time-frequency representations (TFRs) are essential as they provide both time and frequency information simultaneously.

1) Short-Time Fourier Transform (STFT)

Concept:

- STFT breaks a non-stationary signal into small segments using a window function $w(t)$, assuming each segment is approximately stationary.
- Then it applies the Fourier Transform locally.

The STFT partitions the signal into overlapping segments and applies the Fourier Transform to each:

$$\{STFT\}\{x(t)\}(t,\omega) = \int_{\{-\infty\}}^{\{\infty\}x(\tau)w(\tau-t)e^{\{-j\omega\tau\}}d\tau}$$

$x(t)$: input signal
$w(t)$: window function
ω: angular frequency

Derivation:

1. **Windowing**: Multiply the signal $x(\tau)$ with a window w($\tau-t$) cantered at time t.
2. **Fourier Transform** of this windowed segment yields the STFT.

This gives both time and frequency localization, but the resolution is limited:

- Wide window → good frequency resolution, poor time resolution.
- Narrow window → good time resolution, poor frequency resolution.

STFT provides a spectrogram:

$$\{Spectrogram\}(t,\omega) = |\{STFT\}(t,\omega)|^2$$

- This is the **energy density** at each time-frequency point.

Limitation: The time-frequency resolution trade-off is fixed by the choice of window $w(t)$, due to the Heisenberg uncertainty principle

2) Wavelet Transform (WT)

Concept:

- Uses a scaled and shifted version **o**f a function called the mother wavelet $\psi(t)\backslash psi(t)\psi(t)$.
- Allows multi-resolution analysis (time-frequency resolution varies with frequency).

3) Continuous Wavelet Transform (CWT) Formula

$$W_x(a,b) = \frac{1}{\sqrt{|\,a\,|}}\int_{-\infty}^{\infty} x(t)\,\psi^*\left(\frac{t-b}{a}\right)dt$$

To address resolution limitations of STFT, Wavelet Transform uses variable-sized windows.
a: scale (inversely proportional to frequency)
b: translation (time shift)
$\psi(t)$: mother wavelet
$*$: complex conjugate

Derivation:

1. **Scale the wavelet**: $\psi_a(t) = \frac{1}{\sqrt{|a|}}\psi\left(\frac{t}{a}\right)$
2. **Shift the wavelet:** $\psi_{a,b}(t) = \frac{1}{\sqrt{|a|}}\psi\left(\frac{t-b}{a}\right)$

3. **Project the signal** onto this basis:$W_x(a,b) = \langle x(t), \psi_{a,b}(t) \rangle$

This allows high temporal resolution for high-frequency components and high frequency resolution for low-frequency components.

The wavelet transform provides high time resolution at high frequencies and high frequency resolution at low frequencies, making it highly suitable for transient signal detection in condition monitoring Hilbert-Huang Transform (HHT).

HHT consists of two steps:

(1) Empirical Mode Decomposition (EMD):

Decomposes $x(t)$ into a finite number of Intrinsic Mode Functions (IMFs) based on local extrema, without requiring a priori basis functions.

- Each IMF $c_i(t)$ satisfies :
  - The number of extrema and zero-crossings must be equal or differ at most by one.
  - The mean of the upper and lower envelopes (formed by local maxima and minima) is zero.

$$x(t) = \sum_{i=1}^{n} c_i(t) + r_n(t)$$

Process (Iterative):

1. Identify all local maxima/minima.
2. Fit upper and lower envelopes using cubic splines.
3. Subtract mean of envelopes to get a candidate IMF.
4. Repeat "sifting" until IMF conditions are met.
5. Subtract the IMF from the signal and repeat.

(2) Hilbert Transform of IMFs:

For each IMF $c_i(t)$, compute its analytic signal.

$$\hat{x}(t) = \frac{1}{\pi} \text{P} \cdot \text{V} \cdot \int_{-\infty}^{\infty} \frac{x(\tau)}{t-\tau} d\tau$$

Form the analytic signal:

$$z(t) = x(t) + j\hat{x}(t) = A(t)e^{j\phi(t)}$$

where

- $A(t) = \sqrt{x^2(t) + \hat{x}^2(t)}$: Instantaneous Amplitude
- $\phi(t) = \tan^{-1}\left(\frac{\hat{x}(t)}{x(t)}\right)$: Instantaneous Phase

Then, Instantaneous Frequency is given by:

- $f(t) = \frac{1}{2\pi}\frac{d\phi(t)}{dt}$

This time-varying frequency analysis is well-suited for non-linear and non-stationary signals such as those from machinery under variable load or speed.

Application:

- Provides adaptive, data-driven time-frequency-energy representation.
- Excellent for nonlinear and non-stationary signals like machinery vibration under variable speed/load.

III. Materials and Methods

A. For Experimental Setup

The test rig layout, as shown in Fig. 1, incorporates turning machinery ball bearings [7]. Loading is applied in both the axial and radial directions on impaired bearing parts. The rolling element bearings and outer race have been placed in the bearing housing [18]. An accelerometer monitors vibrations by measuring displacement, velocity, and acceleration using a transducer [9]. The displacement transducer has limited effectiveness in monitoring vibrations along the rotating shaft axis caused by defects [11–13]. Load variation was monitored using high-precision strain gauges attached to the bearing housing, ensuring accurate measurement of forces. A mechanical tensioning mechanism was incorporated to regulate the applied load dynamically. The system was calibrated before each test to maintain consistent load conditions. Additionally, real-time monitoring was conducted using LabVIEW software to track load variations and adjust parameters accordingly. The belt-driven system was used to apply radial and axial loads. Load variation was monitored using strain gauges and controlled using tensioning mechanisms. The belt-driven system was used to apply both radial and axial loads on the bearing. Many data collection systems employ signal conditioning techniques to investigate failure frequencies in industrial machinery rolling bearings. When the bearing is connected to the housing, the accelerometer signal is discrete to the frequency range., allowing for high-frequency acceleration measurements. Displacement measurements use a low frequency, while velocity measurements are in the intermediate range. The vibration situation is monitored using an accelerometer with a sensitivity of 10 mV per m/s² and a magnetic base. The test equipment includes a bearing and two shafts with varied speeds. The experimental test rig was constructed and installed on a C-channel frame measuring 584.28×711 mm. The construction of the test rig is designed to minimize the impact of multiple variables, shocks, and vibrations triggered by rotating machinery and equipment. The robust structure is designed for experimental testing under various conditions. The accelerometer's single axis is positioned horizontally inside the bearing housing, with a sensitivity range of 5 to 100 mV. LabVIEW software is used to collect data; fault data is recorded and saved for a specified period, and post-processing is completed using the LabVIEW front end and the necessary hardware. The DAQ system facilitates communication between the user and the computer, providing single-axis values from the accelerometer. The load is applied in line with the belt drive system along the bearing positioned in the test rig. Additionally, the rolling element bearing vibration spectrum is acquired with and without issues over a range of speeds.

The experimental procedure is as follows:

- The national instrument data acquisition system is connected and paired with accelerometers and computer ports for data communication.
- The accelerometer is fixed along the bearing housing.
- Vibration spectrum data is collected while adjusting speed and load.
- The rolling element bearing's vibration signal is recorded and analyzed using waveforms.
- The software analyzes spectrum vibration data using the Fast Fourier Transform approach to determine time and frequency.
- The motor (on the left) drives the pulley, which transfers torque through the belt. The belt drive is connected to the shaft supported by bearings. The tension in the belt generates a radial load on the bearing mounted on the pulley shaft. As shown in Fig. 2(a) the annotations and Fig. 2(b) radial load acting on the bearing.

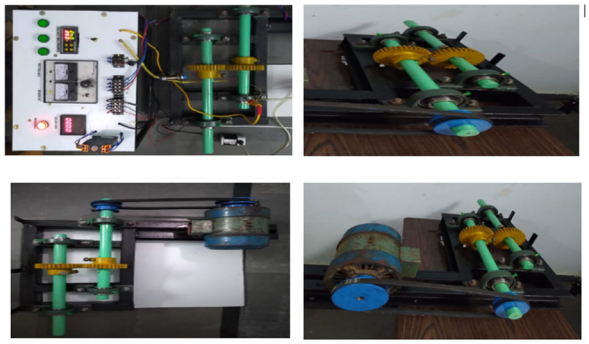

Fig. 1. Layout of the experimental test rig with motor controller.

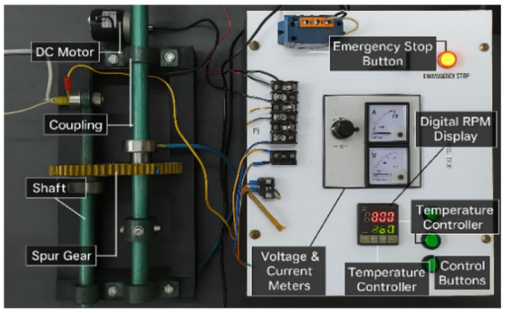

(a)

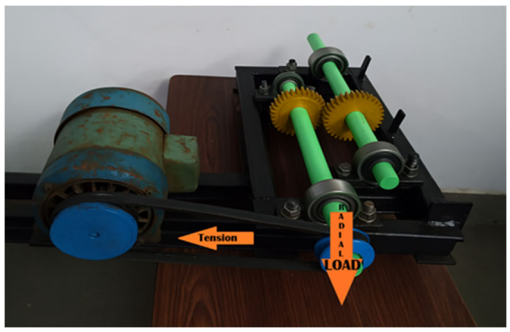

(b)

Fig. 2. (a) Layout with annotations; (b) Tension and Load on the bearing.

The corresponding rolling element analysis for the condition monitoring vibration approach yields various vibration parameters, including RMS, peak-to-peak, zero-to-peak, kurtosis, amplitude, and other factors. Additionally, the signal often contains phase and electrical spikes resulting from changes in the vibration signal's amplitude. The RMS factor is a key measure of the energy content of the vibration signal.

1. **Bearing Specifications**: SKF 6205 deep groove ball bearings.
2. **Test Rig Material Properties**: Constructed from mild steel for structural stability.
3. **Environmental Conditions**: Tests conducted at 25°C with controlled lubrication conditions.

The accelerometer was strategically positioned on the bearing housing at a 45° angle to enhance sensitivity to defect-related vibrations. Finite Element Analysis (FEA) was employed to determine the optimal placement by simulating vibration propagation and response. Additionally, experimental validation was conducted by placing sensors at different positions and analyzing the resulting signal clarity and amplitude. The selected placement ensured maximum defect detection while minimizing interference from external noise. Accelerometer positioned on the bearing housing at 45° to maximize sensitivity to defect-related vibrations. The placement was optimized through Finite Element Analysis (FEA) to identify the most responsive location. Experimental validation confirmed that this orientation captured fault-induced vibrations effectively while minimizing external noise. Accelerometer positioned on the bearing housing at 45° to maximize sensitivity to defect-related vibrations. The placement was optimized using finite element analysis and experimental validation

B. For Tests Conducted in Real-Time at the Sugar Mills Methodology

- After thorough cleaning, the bearing raceways and exterior surfaces, the extent of cage wear, the increase in internal clearance, and the degradation of tolerances were inspected. These areas were carefully examined for any damage or irregularities to determine if the bearing could be reused.
- Testing was carried out using a Multi-Instrument, Piezoelectric Accelerometer, and Data Acquisition System.
- The bearings were examined with greater scrutiny based on their criticality and comparing it with the ISO 20816-3:2022 standard limits.
- The decision to reuse a bearing was made after considering the degree of bearing wear, the machine's function, the bearing's importance in the machine, operating conditions, and the time until the next inspection.
- The equipment tested included Sugar Mill Rollers, Centrifugal Sugar Centrifuges, Conveyors.

A side-by-side comparison of the sample vibration data for scenarios involving 75 HP, 150 HP, and 200 HP motors. Only these (75 HP, 150 HP, and 200 HP motors). These

power ratings were chosen because they were the only machines available for maintenance during the study at the sugar mills Only these (75 HP, 150 HP, and 200 HP motors.) These power ratings were chosen because they were the only machines available for maintenance during the study at the sugar mills, along with the ISO 20816-3:2022 standard limits for rolling element bearings, considering frequencies up to 850 Hz with intervals of 50 Hz shown in Table I and corresponding graph shown in Fig. 3.

To ensure accuracy, the experiments were repeated five times under identical conditions. The results were compared against the ISO 20816-3:2022 standard, and deviation across trials remained within acceptable limits (±5%) [2].

TABLE I. OVERALL MEAN AVERAGE VALUES FOR 12,000 SAMPLE READINGS

Frequency (Hz)	Vibration Velocity (75 HP Motor) (mm/s)	Vibration Velocity (150 HP Motor) (mm/s)	Vibration Velocity (200 HP Motor) (mm/s)	ISO Standard Limit (mm/s)
50	0.21	0.3	0.4	0.7
100	0.31	0.4	0.48	0.7
150	0.38	0.43	0.45	0.7
200	0.33	0.41	0.48	0.7
250	0.34	0.41	0.45	0.7
300	0.41	0.43	0.45	0.7
350	0.38	0.44	0.45	0.7
400	0.38	0.43	0.46	0.7
450	0.4	0.43	0.45	0.7
500	0.41	0.43	0.45	0.7
550	0.4	0.44	0.45	0.7
600	0.4	0.41	0.45	0.7
650	0.4	0.43	0.5	0.7
700	0.4	**0.83**	0.5	0.7
750	0.4	**0.91**	0.5	0.7
800	0.4	**0.95**	0.5	0.7

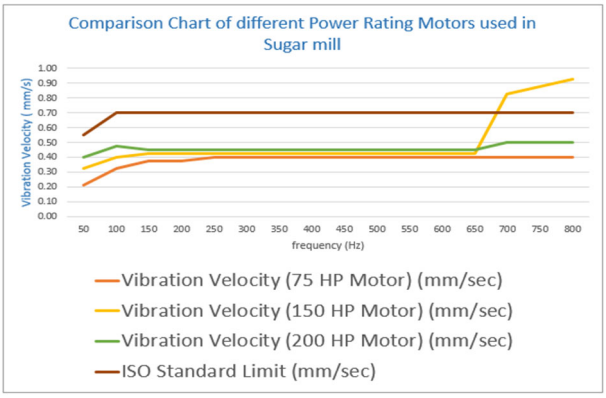

Fig. 3. Overall mean average values for 12,000 sample readings.

IV. RESULT AND DISCUSSION

A. For the Experimental Setup

The frequency domain analysis of roller bearing problems was compared to normal bearings to establish the relationship with fault signals [19]. The equipment operates at speeds ranging from 800 to 1600 rpm. The complete fault signal is captured over a period of 0.2 s. When comparing roller faults to inner and outer race faults, the highest amplitude recorded is 650 Hz. The frequency domain characteristics of normal bearings and overall roller bearing failures vary and change with speed, ranging from 900 to 1600 rpm. Fig. 4 depicts the factors that influence RMS velocity. At 1200 rpm, the frequency is around 200 Hz, but at 1600 rpm, it can reach 700 Hz. In comparison to normal bearings, the frequency range and amplitude of overall roller defects increase. The amplitude of roller defects influences the inner and outer race frequencies, which rise with sidebands [20].

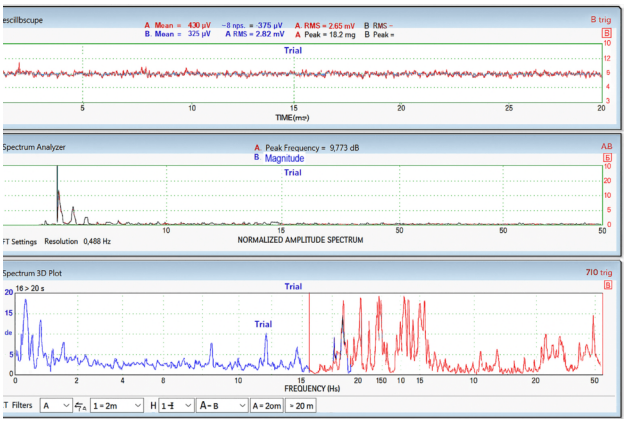

Fig. 4. Time domain analysis for normal bearing.

Damped resonance occurs at frequencies ranging from 350 to 650 Hz. The complete roller bearing defect has a peak-to-peak vibration spectrum ranging from 0.4 µm to 2.5 µm at various speeds. RMS values are greater and vary in frequency from 0.0017 mm/s to 0.0038 mm/s between 115 and 700 Hz, increasing with speed up to 1600 rpm. The frequency distribution includes 95, 125, 250, 350, 480, and 750 Hz. Identifying defects in the frequency domain is rather simple, and particular frequencies may be dynamically added.

However, undesired features, such as noise and other components, might influence the amplitude and excitation frequency [21].

Non-deterministic and non-stationary variables in the vibration signal are recorded across several cycles and frequency ranges. Roller faults exhibit spikiness distributions for frequency and phase angle shift across the total number of cycles [10, 22]. Bearing issues are evaluated and documented in frequency tables for reference. Data for normal and overall roller fault bearings shows varying peak-to-peak frequencies [23]. The primary roller defect is clearly visible in the frequency spectrum, whereas sidebands and distinct harmonics appear at higher frequencies [24, 25]. Wideband noise can influence matching bearing defects and generate resonance in the bearing spectrum. The vibration signal for normal and inner race fault bearings is assessed using time-domain waveform analysis, which is a regular method [26, 27]. For rotational speeds of 800 to 1600 rpm, normal and inner race fault vibration signals were captured for 0.5 s from two successive bearings at sampling speeds of 120 Hz and 180 Hz, respectively.

In this study, vibration spectra were obtained for a predefined set of 15 cases using signals acquired via a

DAQ system. Key parameters—amplitude, kurtosis, and RMS—were used for fault detection and diagnosis of rolling element bearings. The recorded analog signals were digitized using the available data acquisition system and analyzed offline using LabVIEW software at our R&D center.

To minimize noise interference, the following filtering methods were applied

- Band-pass filtering to isolate defect-related frequencies [15].
- Wavelet denoising to enhance fault signal clarity [28].
- FFT-based smoothing to reduce random noise components [24].

Fig. 5 shows vibration spectra for normal and inner race faults. The time-domain spectrum acquired over a specific time frame indicates that the amplitude of inner race defects is much bigger than that of normal bearings [29]. The passing element finds a damped resonance situation in the bearing, which causes defect to excite at a higher frequency [10, 24].

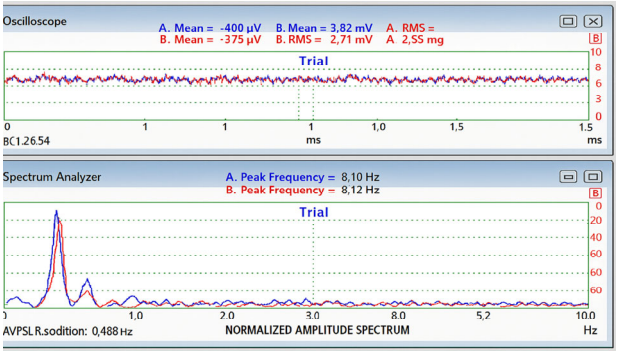

Fig. 5. Oscilloscope and spectrum analyzer graphs for the inner race bearing at 250 Hz.

As a result, the rate of degradation accelerates over time [28]. The nature of strikes and errors is not well-represented in the obtained vibration spectrum, which may contain undesirable components from impulsive impacts in the vibration signal. Obtaining faulty information in the time domain is challenging because the vibration signal receiver captures a sum of dynamic signals over time [16]. Noise and other characteristics are not easily masked in the time domain spectrum. Statistical parameter determination, particularly in the time domain, involves values that are neither deterministic nor stationary, making it difficult to address rolling element bearing issues in the resulting vibration spectrum [10, 24]. Statistical techniques are used to extract parameters in time domain analysis [30], and the output of this vibration signal provides information about the spikiness and overall level of faults in terms of the overall vibration level [31].

The most commonly used approach for time-domain waveform analysis is employed to study vibration signals from both normal and inner race fault bearings. The vibration signal for the normal and inner race fault bearings is captured for 0.5 s from two successive bearings, with sampling rates of around 120 Hz for the normal bearing and 180 Hz for the inner race fault bearing. This examination is performed throughout a rotating speed range of 800 to 1600 rpm. The vibration spectra for the normal and inner race defects reveal significantly distinct patterns, as seen in Fig. 6 below.

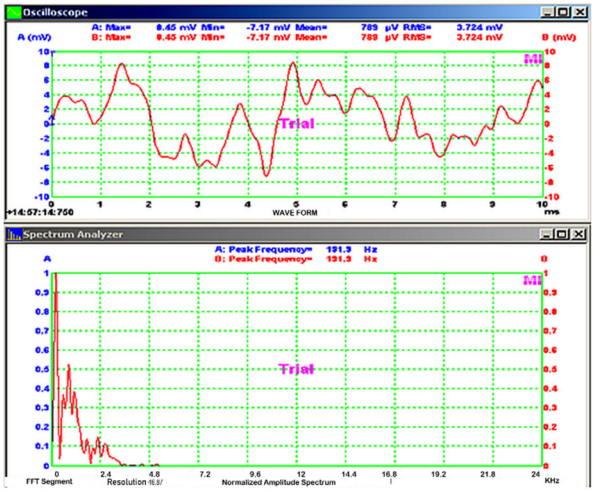

Fig. 6. Study of the spectrum envelope for the inner race bearing at 250 Hz.

Frequency domain analysis revealed outer race faults had the highest amplitudes. Resonance effects and wide-band noise shifted vibration energy, requiring sideband and harmonic analysis for accurate fault detection [32–34]. Envelope detection effectively highlighted defect frequencies.

Figs. 8–11 show spectra and time histories at 250 Hz, confirming that spectral tools are key to isolating fault signatures.

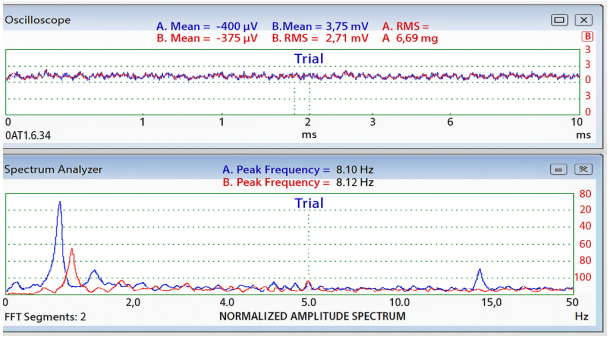

Fig. 8. Oscilloscope and spectrum analyzer graphs for the outer race bearing at 250 Hz.

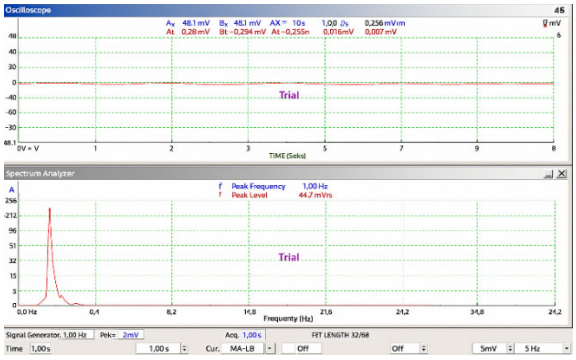

Fig. 9. Spectrum envelope study for the outer race bearing at 250 Hz.

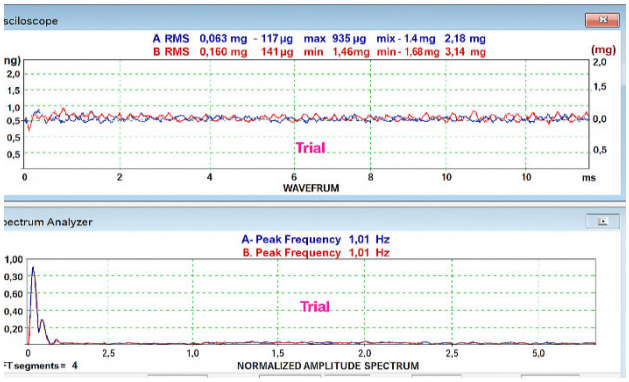

Fig. 10. Oscilloscope and Spectrum Analyser Graphs for the entire bearing at 250 Hz.

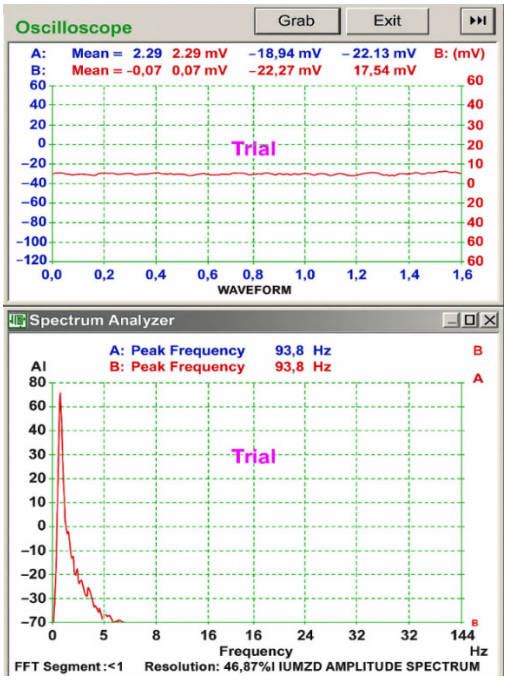

Fig. 11. Spectrum envelope study for the entire bearing at 250 Hz.

B. For Tests Conducted in Real-Time at the Sugar Mills

1) Interpretation

- The data chart compares the vibration velocity data for 75 HP, 150 HP, and 200 HP motors, with the ISO standard limits for rolling element bearings.
- In all scenarios except for the 150 HP motor. The defect in the 150 HP motor is evident by the increased vibration velocities between 700 Hz and 850 Hz, which exceed the ISO standard limits.

2) Action

- Immediate action is warranted for the 150 HP motor scenario with the defect. Maintenance and diagnostic procedures should be conducted to identify and rectify the underlying cause of the increased vibration levels to ensure the reliable operation of the equipment.
- The 75 HP and 200 HP motors exhibit acceptable vibration levels within the ISO standard limits and do not require immediate action. Regular monitoring and maintenance should still be conducted to ensure continued reliability.

C. Overcoming a Bearing Defect in a 150 HP Motor

- Inspection: Identify the type of defect in the bearing, such as wear due to insufficient lubrication.
- Lubricant Selection: Choose a high-performance grease with the correct viscosity.
- Manual Greasing: Apply the recommended amount of grease using a grease gun, ensuring even distribution.
- Automatic Lubricator: Install an automatic lubricator to maintain consistent lubrication.
- Condition Monitoring: Implement vibration analysis to monitor bearing condition and detect any further issues.
- Table II shows a comparison of Detection rate and False Alarm Rate for Each method.

TABLE II. COMPARING DETECTION RATE (%) AND FALSE ALARM RATE (%) FOR EACH METHOD

Method	Detection Rate (%)	False Alarm Rate (%)
Time Domain Analysis	85	12
Frequency Domain Analysis	90	10
Spectrum Plot Approach	95	7
Traditional Vibration (RMS)	78	15

A re-test was done after maintenance for 150 HP motor the results are shown in Table III and Fig. 12.

TABLE III. OVERALL MEAN AVERAGE VALUES FOR 12,000 SAMPLE READINGS

Frequency (Hz)	150 HP Motor (mm/s)	ISO 20816-3:2022 Limit (150 HP ≤) (mm/s)
50	0.15	1.2
100	0.25	1.2
150	0.35	1.2
200	0.45	1.2
250	0.55	2
300	0.65	2
350	0.75	2
400	0.85	2
450	0.95	2
500	1.05	3.2
550	1.15	3.2
600	1.25	3.2
650	1.35	3.2
700	1.45	3.2
750	1.55	3.2
800	1.65	3.2
850	1.75	3.2

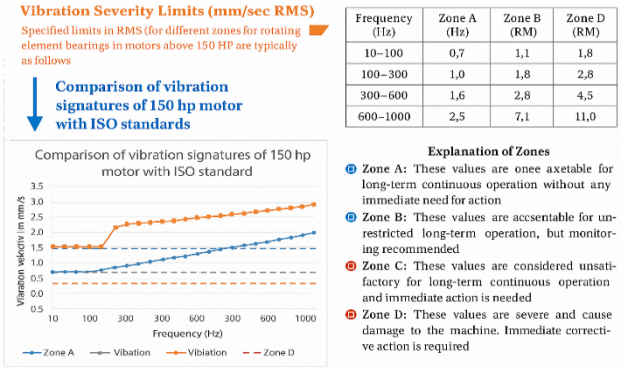

Fig. 12. Comparison data with ISO standard.

The 1 HP motor setup limits industrial relevance. Future work will include high-power motors, adaptive signal processing, and AI-based diagnostics.

V. Conclusion

The study explored a multi-domain approach for diagnosing faults in rolling element bearings, focusing on time-domain, frequency-domain, and spectrum plot analyses. Each method offered distinct advantages and limitations when applied to experimental data collected from both a custom-built test rig and real-time industrial setups, such as sugar mill machinery.

In the time-domain analysis, statistical parameters such as RMS, kurtosis, and peak values were computed. While this approach allowed for basic fault detection, the clarity of the results was limited due to the presence of noise and impulsive components that masked subtle fault signatures. The inability to isolate specific frequencies made it less reliable for early fault identification, particularly in complex operating environments.

Frequency-domain analysis, on the other hand, enabled clearer visualization of defect frequencies, especially those related to outer and inner race faults. The shift in dominant frequencies and increase in amplitude under faulty conditions confirmed the diagnostic value of spectral techniques. The presence of sidebands and harmonic components helped in pinpointing defect locations and understanding their severity.

Among the methods evaluated, spectrum plot analysis showed the highest diagnostic accuracy. This approach not only captured variations in signal amplitude and frequency but also highlighted damped resonance and wideband noise effects, which are critical in assessing progressive damage. The spectrum plots consistently revealed fault signatures that were not easily observable in the time domain, making this method particularly effective in early fault detection and condition monitoring.

The real-time validation at sugar mills, involving 75 HP, 150 HP, and 200 HP motors, further strengthened the practical relevance of the approach. Vibration data exceeding ISO 20816-3:2022 limits in the 150 HP motor confirmed a bearing defect, which was subsequently mitigated through targeted maintenance. Post-maintenance results showed significant improvement, validating the diagnostic framework used in this study.

Overall, the integration of experimental data, advanced signal processing techniques, and comparative domain analyses provided a holistic understanding of bearing fault behaviour's. The findings highlight the superiority of spectrum plot methods over traditional time-domain analysis, offering a more reliable and adaptable solution for real-time industrial applications.

Conflict of Interest

The authors declare no conflict of interest.

Author Contributions

Vinayak Kulkarni: Conducted case studies and experimental validations for vibration analysis techniques. Dr. Shylesha Channapattana: Supervised the research framework, provided expert guidance, and reviewed the manuscript for accuracy and coherence. All authors had approved the final version.

Acknowledgment

The author wishes to thank Dr. Shylesha Channapattana for Guiding this research work.

References

[1] P. Gupta and M. K. Pradhan, "Fault detection analysis in rolling element bearing: A review," *Mater. Today: Proc.*, vol. 4, no. 2, pp. 2085–2094, 2017. doi: 10.1016/j.matpr.2017.02.054

[2] A. Khadersab and S. Shivakumar, "Vibration analysis techniques for rotating machinery and its effect on bearing faults," *Procedia Manuf.*, vol. 20, pp. 247–252, 2018. doi: 10.1016/j.promfg.2018.02.036

[3] H.-Q. Wang *et al.*, "Fault detection enhancement in rolling element bearings via peak-based multiscale decomposition and envelope demodulation," *Adv. Mech. Eng.*, vol. 2014, 329458, 2014. doi: 10.1155/2014/329458

[4] C. Vale *et al.*, "Novel efficient technologies in Europe for axle bearing condition monitoring—the MAXBE project," *Transp. Res. Procedia*, vol. 14, pp. 635–644, 2016. doi: 10.1016/j.trpro.2016.05.313

[5] S. Alegranzi, J. F. Gonçalves, and H. Gomes, "Ball bearing vibration monitoring for fault detection by the envelope technique," *Procedia CIRP*, vol. 17, pp. 4113–4125, 2014. doi: 10.5151/meceng-wccm2012-19745

[6] P. Bagiński and G. Zywica, "The influence of temperature on dynamics of the rotor—Foil bearing system," *Mechanik*, vol. 63, pp. 634–635, 2016. doi: 10.17814/mechanik.2016.7.103

[7] V. Kulkarni and A. Khadersab, "Condition monitoring analysis of rolling element bearing based on frequency envelope," *Mater. Today: Proc.*, vol. 46, pp. 4667–4671, 2021. doi: 10.1016/j.matpr.2020.10.291

[8] A. Khadersab and S. Shivakumar, "Vibration analysis techniques for rotating machinery and its effect on bearing faults," *Mater. Today: Proc.*, vol. 20, pp. 247–252, 2018. doi: 10.1016/j.promfg.2018.02.036

[9] A. Moshrefzadeh, "Condition monitoring and intelligent diagnosis of rolling element bearings under constant/variable load and speed conditions," *Mech. Syst. Signal Process.*, vol. 149, 107153, 2021. doi: 10.1016/j.ymssp.2020.107153

[10] S. Wei, J. Wang, and J. Ou, "Method for improving the neural network model of the magnetorheological damper," *Mech. Syst. Signal Process.*, vol. 149, 107316, 2021. doi: 10.1016/j.ymssp.2020.107316

[11] D. Wang, P. W. Tse, and K. L. Tsui, "An enhanced kurtogram method for fault diagnosis of rolling element bearings," *Mech. Syst. Signal Process.*, vol. 35, no. 1–2, pp. 176–199, 2013. doi: 10.1016/j.ymssp.2012.10.003

[12] D.-T. Hoang and H.-J. Kang, "Rolling element bearing fault diagnosis using convolutional neural network and vibration image," *Cognit. Syst. Res.*, vol. 53, pp. 42–50, 2019. doi: 10.1016/j.cogsys.2018.03.002.

[13] Z. Liu *et al.*, "A study of a speed amplified linear generator for low-frequency wave energy conversion," *Mech. Syst. Signal Process.*, vol. 149, Art. no. 107226, 2021. doi: 10.1016/j.ymssp.2020.107226

[14] A. Skariah *et al.*, "Health monitoring of rolling element bearings using improved wavelet cross spectrum technique and support vector machines," *Tribol. Int.*, vol. 154, 106650, 2021. doi: 10.1016/j.triboint.2020.106650

[15] X. Rui *et al.*, "Design and analysis of a broadband three-beam impact piezoelectric energy harvester for low-frequency rotational motion," *Mech. Syst. Signal Process.*, vol. 149, 107307, 2021. doi: 10.1016/j.ymssp.2020.107307

[16] T. Berredjem and M. Benidir, "Bearing faults diagnosis using fuzzy expert system relying on an improved range overlaps and similarity method," *Expert Syst. Appl.*, vol. 108, pp. 134–142, 2018. doi: 10.1016/j.eswa.2018.04.025

[17] B. A. Tama, M. Vania, and S. Lee, "Recent advances in the application of deep learning for fault diagnosis of rotating machinery using vibration signals," *Artif. Intell. Rev.*, vol. 56, pp. 4667–4709, 2023. doi: 10.1007/s10462-022-10293-3

[18] I. Antoniadou *et al.*, "A time–frequency analysis approach for condition monitoring of a wind turbine gearbox under varying load conditions," *Mech. Syst. Signal Process.*, vol. 64–65, pp. 188–216, 2015. doi: 10.1016/j.ymssp.2015.03.003

[19] D. Liu, W. Cheng, and W. Wen, "Rolling bearing fault diagnosis via STFT and improved instantaneous frequency estimation method," *Procedia Manuf.*, vol. 49, pp. 166–172, 2020. doi: 10.1016/j.promfg.2020.07.014

[20] L. Hu *et al.*, "Extraction of the largest amplitude impact transients for diagnosing rolling element defects in bearings," *Mech. Syst. Signal Process.*, vol. 116, pp. 796–815, 2019. doi: 10.1016/j.ymssp.2018.07.022

[21] J. Zhou, W. Sun, and L. Cao, "Vibration and noise characteristics of a gear reducer under different operation conditions," *J. Low Freq. Noise Vib. Act. Control*, vol. 38, no. 2, pp. 574–591, 2019. doi: 10.1177/1461348419825603

[22] W. Wang, B. D. Forrester, and P. C. Frith, "A unified approach to detecting and trending changes caused by mechanical faults in rotating machinery," *Struct. Health Monit.*, vol. 15, no. 2, pp. 204–222, 2016. doi: 10.1177/1475921716636337

[23] H. Saruhan *et al.*, "Vibration analysis of rolling element bearings defects," *J. Appl. Res. Technol.*, vol. 12, no. 3, pp. 384–395, 2014. doi: 10.1016/S1665-6423(14)71620-7

[24] A. Mauricio and K. Gryllias, "Cyclostationary-based multiband envelope spectra extraction for bearing diagnostics: The combined improved envelope spectrum," *Mech. Syst. Signal Process.*, vol. 149, 107150, 2021. doi: 10.1016/j.ymssp.2020.107150

[25] Z. Kıral and H. Karagülle, "Vibration analysis of rolling element bearings with various defects under the action of an unbalanced force," *Mech. Syst. Signal Process.*, vol. 20, no. 8, pp. 1967–1991, 2006. doi: 10.1016/j.ymssp.2005.05.001

[26] X. Yan, Y. Liu, and M. Jia, "A feature selection framework-based multiscale morphological analysis algorithm for fault diagnosis of rolling element bearing," *IEEE Access*, vol. 7, pp. 123436–123452, 2019. doi: 10.1109/ACCESS.2019.2937751

[27] R. K. Jha and P. D. Swami, "Fault diagnosis and severity analysis of rolling bearings using vibration image texture enhancement and multiclass support vector machines," *Appl. Acoust.*, vol. 182, 108243, 2021. doi: 10.1016/j.apacoust.2021.108243

[28] P. S. Kumar, S. K. Laha, and L. A. Kumaraswamidhas, "Assessment of rolling element bearing degradation based on dynamic time warping, kernel ridge regression and support vector regression," *Appl. Acoust.*, vol. 208, 109389, 2023. doi: 10.1016/j.apacoust.2023.109389

[29] Z. Ni *et al.*, "Bearing inner race fault detection and size estimation using the variable reluctance sensor," *J. Sound Vib.*, vol. 530, 116968, 2022. doi: 10.1016/j.jsv.2022.116968

[30] J. Millet-Roig *et al.*, "Study of frequency and time domain parameters extracted by means of wavelet transform applied to ECG to distinguish between VF and other arrhythmias," *Comput. Cardiol.*, vol. 25, pp. 17–20, 1998. doi: 10.1109/CIC.1998.731698

[31] P. H. Jain and S. P. Bhosle, "A review on vibration signal analysis techniques used for detection of rolling element bearing defects," *SSRG Int. J. Mech. Eng.*, vol. 8, no. 1, pp. 14–29, 2021. doi: 10.14445/23488360/IJME-V8I1P103

[32] X. Rui *et al.*, "Design and analysis of a broadband three-beam impact piezoelectric energy harvester for low-frequency rotational motion," *Mech. Syst. Signal Process.*, vol. 149, 107307, 2021. doi: 10.1016/j.ymssp.2020.107307

[33] D. Kuzio, R. Zimroz, and A. Wyłomańska, "Identification of fault frequency variation in the envelope spectrum in the vibration-based local damage detection in possible changing load/speed conditions," *Measurement*, vol. 218, 113148, 2023. doi: 10.1016/j.measurement.2023.113148

[34] A. Hu *et al.*, "Frequency loss and recovery in rolling bearing fault detection," *Chin. J. Mech. Eng.*, vol. 32, 35, 2019. doi: 10.1186/s10033-019-0349-3